RAM ROBOTICS AND MECHATRONICS

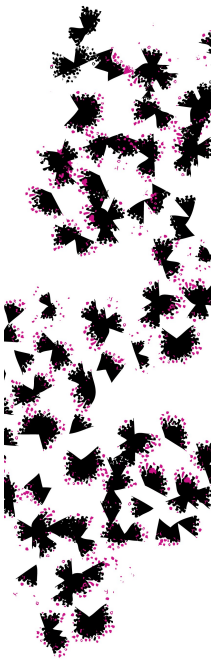

Controller Design of a Variable Stiffness Joint for Catching a Moving Object

J. (Julian) Kumle

Individual Assignment

Committee:
Dr. R. Carloni
S.S. Groothuis, MSc

December 2015

036RAM2015
Robotics and Mechatronics
EE-Math-CS
University of Twente
P.O. Box 217
7500 AE Enschede
The Netherlands

UNIVERSITY OF TWENTE.

MIRA CTIT
BIOMEDICAL TECHNOLOGY AND TECHNICAL MEDICINE

Controller Design of a Variable Stiffness Joint for Catching a Moving Object

J. Kumle, S.S. Groothuis and R. Carloni

Abstract— **In this paper a control method is designed in order to catch a moving object by means of a robotic joint that implements a variable stiffness actuator (VSA). The controller acts as a virtual damper for absorbing the kinetic energy of the object. The gain of the virtual damping and the physical stiffness of the VSA are the control variable. To obtain a critically damped system the damping gain is scheduled on both, the physical stiffness and the inertia of the system. By changing the stiffness of the VSA, the internal deflection of the VSA can be controlled. Experiments on the rotational variable stiffness actuator vsaUT-II validate the principal functionality of the method.**

I. INTRODUCTION

If a human catches an object different parts of the human has to interact perfectly. First, the movement of the object is observed and an location as well as a point of time is determined for catching the object. The arm muscles are pre-tensioned for preparing the arm to the momentum the object will transfer to the arm. As soon as the arm gets in contact with the object the muscles are tensioned for absorbing the kinetic energy of the object. Figure 1a and figure 1b show a manikin catching a falling ball. In figure 1a the manikin does not tense the arm muscles which results in a big deflection of the elbow. In figure 1b the manikin does tense the arm muscles and therefore decreases the deflection.

The objective of this paper is to control a one degree of freedom actuator for catching an object by imitating the behaviour of an human arm, as shown in figure 1a and figure 1b. An additionally objective is that the actuator interacts safely in a human environment. Using a *Variable Stiffness Actuator (VSA)* presents the opportunity to adapt the stiffness of the actuator during the catching process as the human is able to tense the muscles of the arm. The controller in this paper is implemented as a virtual damper in order to absorb the kinetic energy of the moving object. The paper focuses on controlling the deflection of the VSA. Therefore the stiffness of the VSA gets adjusted to control the maximum deflection dependent on the estimated total energy of the system. The damping gain of the virtual damper get scheduled on the inertia and the stiffness of the elastic element for achieving a desired oscillation behaviour. The moving object is not detected before it collides with the VSA output. Therefore, it is assumed that the object has always the same trajectory and gets in contact with the VSA at the same position.

This work was funded by the European Commissions Seventh Framework Programme as part of project SHERPA under grant no. 600958.

The authors are with the Faculty of Electrical Engineering, Mathematics and Computer Science, University of Twente, The Netherlands. Email: j.kumle@student.utwente.nl, {s.s.groothuis, r.carloni}@utwente.nl

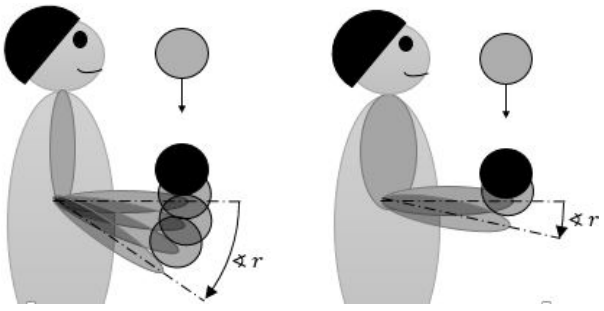

(a) Arm muscles are not tensed (b) Arm muscles are tensed

Fig. 1: Catching a dropping object without tension in the arm and with tensed arm.

Furthermore, it is assumed that the mass of the moving object is known and a mechanism is implemented at the VSA that rigidly attaches the object to the VSA output after collision.

The literature research is structured in three topics. First, safely interacting with the environment can be realized by a compliant actuation. [1], [2] and [6] are using an impedance control for obtaining a compliant actuation. As in [6] the controller in this paper is tuned by considering the controller motor combination as virtual mechanical elements, define the target dynamics of a pure mechanical system and choose the control gains for achieving these defined target dynamics. Compared to the mentioned papers the controller in this paper is acting as a pure damper and therefore only absorbs energy. Second, in order for catching a moving object a damping element, which absorbs the kinetic energy in the system, is required. In [7], [8] and [9] damping injections are represented. As in [9] the damping gain in this paper is scheduled on both, the stiffness and the inertia of the system but compared to the mentioned papers the control gains are scheduled on the target dynamics of a linearised system with respect to the limitations of the system. The last topic describes different control methods and applications of VSAs which can be found in [3], [4], [5] and [10]. As in [3] a gain scheduling is performed on a VSA within this paper but compared to the mentioned paper this controller is designed as a virtual damper for catching a moving object.

The paper is structured as follows:

- I Introduction
- II Controller Design
- III Experiments and Results
- IV Discussion
- V Conclusion
- VI Appendix

II. Controller Design

In this section, the design of a controller for a variable stiffness actuator is presented.

VSAs have the advantage that their output stiffness at the output can be changed independently from the output position. In this paper a VSA is considered which consists out of two internal motors, an elastic element and an output where a load can be connected to as shown in figure 2. First motor tunes the stiffness $K(q_1)$ of the elastic element by its output position q_1 to the demands of the application. Second motor controls the output position of the VSA while the motor is connected to the output via the elastic element. Let r be the absolute angular position of the output link with respect to the frame and q_2 the absolute angular position of the motor with respect to the frame. Additionally, the inertia J_{load} of the VSA output is an important parameter for analysing and controlling the behaviour of the system.

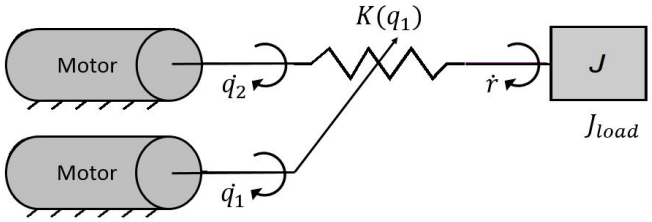

Fig. 2: Illustration of a variable stiffness actuator, where J is the load connected to the output represented by a inertia, $K(q_1)$ is the stiffness of the elastic element and $\dot{q_1}, \dot{q_2}, r$ are angular velocities. The frame represents the fixed world

A. Desired behaviour and control goals

An object with a known mass moves with a certain velocity towards the output of the VSA. In this paper it is assumed that a mechanism rigidly attaches the objects to the VSA output as soon as the object gets in contact with the output. If the object is rigidly connected to the VSA output the inertia of the output increases. If the momentum of the moving object is transformed by an elastic collision to the VSA output kinetic Energy is stored in the system and the output starts moving, $\dot{r} \neq 0$. A movement of r leads to a deflection of the elastic element and therefore potential energy are saved in the VSA. During this step energy gets transferred from kinetic energy E_{kin} into potential energy E_{pot}. If the potential energy gets larger than the kinetic energy $E_{pot} > E_{kin}$ the object accelerates in the opposite direction of the original movement of the object. Due to the goal of stopping the object a change of direction should be avoided. For safely interacting with the environment a compliant character can be achieved by a low stiffness of the VSA. The deflection of r to its equilibrium position should stay small. With respect to the described desired behaviour, the following control goals are defined:

- $\lim_{t \to t_f} \dot{r}(t) = 0$
- $E_{pot}(t) \leq E_{kin}(t), \forall t \in [0, t_f]$
- $K(q_1, t)$: low $\forall t \in [0, t_f]$
- $|r(0) - r(t)|$: small $\forall t \in [0, t_f]$

B. Control architecture

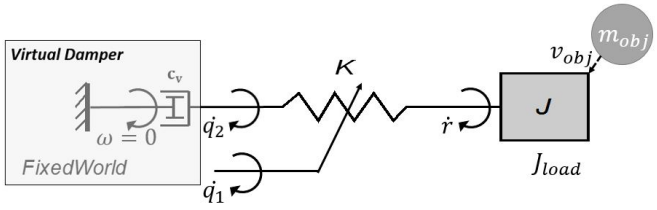

Fig. 3: Illustration of a virtual damper with the damping gain c_v replacing the motor for changing q_2 in order to design a controller that act as a damper. Motor for changing q_1 is irrelevant for that part and therefore taken out of the sketch.

The first control goal $\lim_{t \to t_f} \dot{r}(t) = 0$ defines that the kinetic energy of the system should be absorbed. For absorbing kinetic energy the controller-motor combination is considered as a virtual damper which is connected to the fixed world. Figure 2 can be redrawn to figure 3, where the motor for changing q_2 is sketched as a damper with the damping constant c_v connecting q_2 to the fixed world. The circle in the figure represents the moving object, which should be caught. The parameter for the moving object is its mass m_{obj} and its velocity v_{obj}. If the object gets in contact with the VSA output the rule for conservation of momentum defines the rotating speed of r by the formula $\dot{r} = \frac{m_{obj} v_{obj}}{J}$. The VSA output accelerates according to $\ddot{r} = \frac{\partial \dot{r}}{\partial t}$. This acceleration creates an impulsive torque to the output which is transferred to the elastic element.

On the basis of the illustration in figure 3 a block diagram as seen in figure 4 can be drawn. The impulsive torque input M_{obj} is modelled by two step sources subtracted from another, where the second has the same final value as the first with a step time difference of $\Delta t = 10$ms what results in a pulse with duration of Δt. Figure 4 shows that the Controller, as virtual damper, is a proportional controller with a gain of $\frac{1}{c_v}$. The input of the controller is the torque τ_s saved in the elastic element which results out of the position difference $q_2 - r$ and the stiffness $K(q_1)$ of the elastic element. The output of the controller is a target velocity $\dot{q}_2$ for the motor. The velocity of the VSA output $\dot{r}$ results out of the torque τ_s saved in the elastic element and the impulsive torque input M_{obj} acting on the inertia of the VSA output.

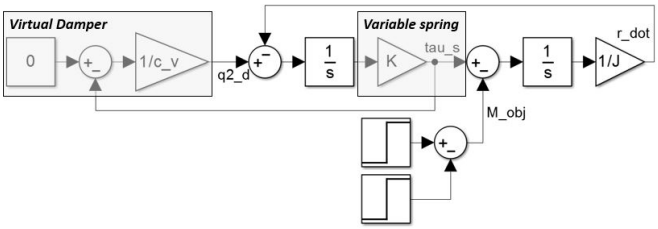

Fig. 4: Block diagram based on the illustration of figure 3. Figure represents the general control architecture.

C. Adapting the stiffness of the elastic element

For interacting safely with the environment and human beings compliant actuation can be realized by a low stiffness $K(q_1)$ of the elastic element inside the VSA. The stiffness of the elastic element is a function of q_1. Due to Hooke's Law the energy of the elastic element depends on the stiffness of the elast element $K(q_1)$ and the deflection $(r-q_2)$. Therefore the most compliant stiffness for a defined maximum deflection can be calculated by a defined maximum deflection and the total energy in the system, shown in equation (4). The total energy in the system is the sum of the kinetic energy and the potential energy. The kinetic energy in the system can be calculated by the inertia of the system and the velocity of the VSA output. The energy functions are shown in equations (1),(2) and (3).

$$E_{pot} = \frac{1}{2}K(q_1)(r-q_2)^2 \tag{1}$$

$$E_{kin} = \frac{1}{2}J\dot{r}^2 \tag{2}$$

$$E_{total} = E_{pot} + E_{kin} \tag{3}$$

$$K_{des} = \frac{E_{total}}{2d_{max}} \tag{4}$$

Since the stiffness $K(q_1)$ is a function of q_1 a desired stiffness of the elastic element defines a desired q_1. This leads to a position controller on q_1, shown in figure 5. The first block transfers a desired stiffness K_{des} into a desired position of the pivot point $q_{1_{desired}}$. After this block there is a closed loop containing the position controller and the plant of the system. The output of the plant is the position of q_1 which leads to the stiffness of the elastic element.

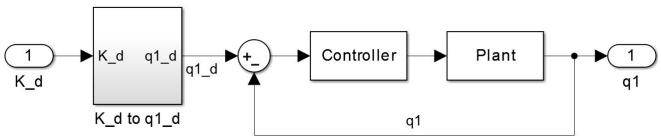

Fig. 5: Position control on q1 for achieving $K_{desired}$

.

D. Choose damping gain

The control goal $E_{pot}(t) \leq E_{kin}(t), \forall t \in [0, t_f]$ defines that overshoot of r should be avoided and because of the control goal $|r(0)-r(t)|$: small $\forall t \in [0, t_f]$ a critical damped system is required.

By analysing the block diagram in figure 4 a transfer function from the momentum of the moving object M_{obj} to the velocity of the VSA output $\dot{r}$ can be created. Shown in equation (5).

$$\frac{\dot{r}}{M_{obj}} = \frac{1}{J}\frac{s+\frac{K}{c_v}}{s^2+s\frac{K}{c_v}+\frac{K}{J}} \tag{5}$$

$$T = \frac{Y}{U} = \frac{K\omega^2}{s^2+2\zeta\omega s+\omega^2} \tag{6}$$

The transfer function of the system, shown in (5) is of order two and compared to the standard transfer function of a second-order systems, shown in equation (6), the undamped angular frequency ω can be calculated, as shown in equation (7).

$$\omega = \sqrt{\frac{K}{J}} \tag{7}$$

By using the natural frequency and the transfer function for the standard form of a second-order system the damping ratio of the system ζ can be determined by the formula (9), which results out of equation (8. The gain for the virtual damper results out of a desired damping ratio, shown in equation (10). The damping ratio ζ describes the damping behaviour of the system.

- $\zeta < 1$ - under-damped system
- $\zeta = 1$ - critically damped system
- $\zeta > 1$ - over-damped system

$$2\zeta\omega = \frac{K}{c_v} \tag{8}$$

$$\zeta = \frac{K}{2c_v\omega} = \frac{K}{2c_v\sqrt{\frac{K}{J}}} = \frac{\sqrt{KJ}}{2c_v} \tag{9}$$

$$c_v = \frac{\sqrt{KJ}}{2\zeta} \tag{10}$$

Because a variable stiffness actuator can vary the stiffness of the elastic element $K(q_1)$ the damping factor is scheduled on both the stiffness and the inertia of the System.

III. Experiments and Results

In this paper the method is applied on the vsaUT-II, a rotational variable stiffness actuator [12], shown in figure 6.

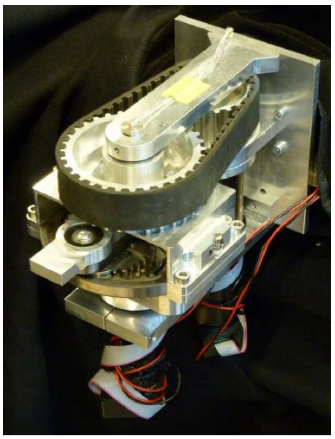

Fig. 6: Picture of the vsaUT-II [12].

A. Experimental set-up

The VSA contains a motor-transmission combination for changing q_1 and q_2. A non-linear relation leads from the position of r, q_2 and q_1 to the stiffness of the elastic element explained by equation (11), where k is the elastic constant for the internal elastic elements and L is the lever arm length. Along the lever arm a pivot point q_1 can be moved for changing the stiffness of the elastic element from 0.7 Nm/rad to 400 Nm/rad. An initial stiffness of 1Nm/rad was chosen so that the natural frequency of the system ω is smaller than the crossover frequency of the system w_c for changing the position of q_2 and therefore being able to follow the movement of r. Due to mechanical end-stops of the system q_2 can move from $-0.5...0.5$ rad and r can move dependent of the position of q_2 from $q_2 - 0.7$ rad$...q_2 + 0.7$ rad. Further important values for implementing the controller are shown in tables I - III.

$$K := \frac{\partial \tau_r}{\partial r} = 2kL^2 \frac{(L - q_1)^2}{q_1^2} \cos(2(r - q_2)) \qquad (11)$$

TABLE I: Parameters for the path of q_1.

max. motor speed	872 [rad s]
max. continuous torque	0.0263 [Nm]
stall torque	0.243 [Nm]
speed reduction ratio	0.0022 [−]
motor shaft inertia	$1.07 \cdot 10^{-6}$ [kg m^2]
motor friction	$6.4 \cdot 10^{-6}$ [Ns/m]
transmission input inertia	$4 \cdot 10^{-8}$ [kg m^2]
max. transmission efficiency	0.59 [−]

TABLE II: Parameters for q_2.

max. motor speed	726 [rad/s]
max. continuous torque	0.17 [Nm]
stall torque	2.28 [Nm]
speed reduction ratio	0.0044 [−]
motor shaft inertia	$1.38 \cdot 10^{-5}$ [kg m^2]
motor friction	$3 \cdot 10^{-6}$ [Ns/m]
transmission input inertia	$9.1 \cdot 10^{-7}$ [kg m^2]
max. transmission efficiency	0.72 [−]

TABLE III: Parameters for the bath between q_2 and r.

friction	$1.2 \cdot 10^{-}2$ [Ns/m]
inertia	$1.1 \cdot 10^{-}2$ [kg m^2]

The parameters, shown in tables I - III are used for creating a simplified plant on which the control method can be tested. The simplified model was validated by comparing it to a complex model of the system described in [12].

Additionally a magnet was mounted to the VSA output for attaching the object rigidly to the output. The object is an iron ring, with a weight of $m_{obj} = 0.108$ kg rolling down from a ramp before hitting the output. The iron ring hits the output at $t = 1$ s. If the iron ring is connected to the output the inertia of the VSA output changes to 0.0205 kg m^2. The height of the ramp is 0.3 m and therefore the velocity can be calculated by considering the energy. The experimental set-up is schematic shown in figure 7, where (1) is the object rolling down from the ramp (2) and hitting the magnet (3) which is rigidly connected to the output (4) of the VSA (5).

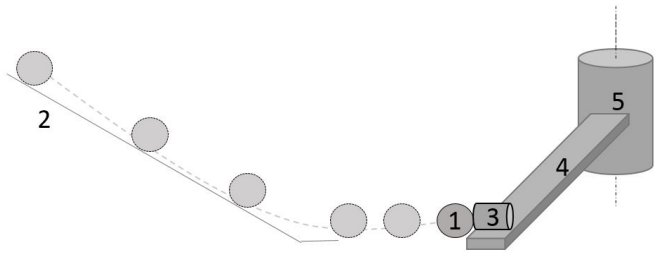

Fig. 7: Schema of experimental set-up. Where (1) is the object rolling down from the ramp (2) and hitting the magnet (3) which is rigidly connected to the output (4) of the VSA (5).

The VSA is equipped with three position sensors for measuring q_1, q_2 and r. An Adruino μ-Controller communicates to the sensors and actuators. This μ-Controller has an interface to Matlab-Simulink so that the controller can be implemented in Matlab-Simulink. The motor controller for q_1 and q_2 are ELMO Whistle controllers.

The limitations of the system are the end-stops of q_2 and r and the maximum motor speed of q_1 and q_2. The end-stops limit the movement of the VSA output. The maximum motor speed for q_2 limits the maximum damping factor of the virtual damper and the maximum motor speed for q_1 limits the rate of change for the stiffness of the elastic element. The experiments described in this paper were performed within the limitations of the system.

B. Results

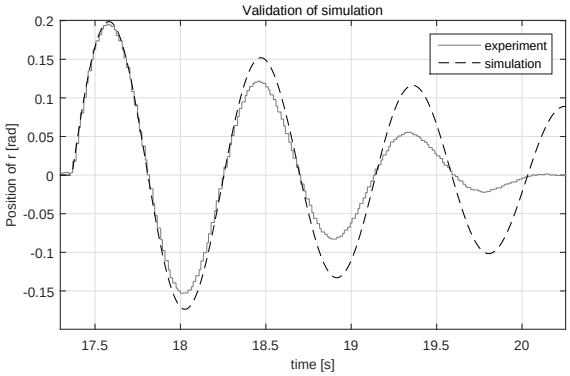

Fig. 8: Validation of simulation on experimental set up at an uncontrolled system. The iron ring hits the VSA output at $t = 17.3$ s

.

After setting up the controller and applying the described method in section II simulations and experiments were performed. First, the behaviour of the uncontrolled system of the experimental set up was compared to the simulation at a stiffness of 1 Nm/rad while the virtual damper was inactive

($\dot{q_2} = 0$ rad/s, $\forall t \in [0, t_f]$). The results are shown in figure 8. While the simulation and the experiment show similar oscillation behaviour, differences in the damping behaviour can be seen. For the simulation a simplified friction model by a constant friction gain is modelled which leads to these differences. The validation of the simulation model shows a sufficient result for implementing and testing the controller in a simulation before applying it at the experimental set up.

The second experiment, shown in figure 9, was performed by implementing the virtual damper. The behaviour of the damped system is compared to the undamped system (dotted line). The behaviour of a critically damped system was analysed at the experimental set up (dashed line) and in a simulation (solid line). The stiffness of the elastic element is constant at 1 Nm/rad during this experience. A damping ratio of $\zeta = 1$ results in a damping gain for the virtual damper of 0.071 Ns/m. The plot on the top shows the movement of r. The plot in the middle shows the movement of q_2. The plot at the bottom shows the motor activity for changing q_2. In the experiment q_2 reacts on the requested motor speed slower than in the simulation. Likely this is the case due to a time delay within the communication between Matlab-Simulink, μ-controller and motor controllers. Due to a slower reaction of q_2 in the experiment the deflection of r and q_2 is greater, a greater deflection leads to a greater force in the elastic element counteracting the movement of r and therefore the total deflection of r to its equilibrium point is smaller. No overshoot of r can be detected and the system is indeed close to being critically damped. The result of the experiment and the simulation of the controlled system show the desired behaviour described in section II and fulfil the control goals.

Varying the gain of the virtual damper should has an influence on the damping ratio. Therefore experiments were performed with slightly changed damping gains and the behaviour is compared to the critically damped system.

Figure 10 compares the gain for the critically damped system with a gain for a slightly over-damped system. In the experiment and at the simulation a higher damping ratio request a faster change of q_2 and therefore a smaller force counteracts the movement of r. As in the last experiment q_2 reacts slower in the experimental set up than in the simulation which leads to a smaller total deflection of r to its equilibrium point at the experimental set up.

Figure 11 compares the gain for the critically damped system with a gain for a slightly under-damped system. The results of the experimental set up show a clear overshoot for r, whereas a close look is needed to see the overshoot in the simulation. Again, the difference between the simulation and the experimental set up regarding the deflection are obvious.

Furthermore, a simulation was performed for changing the maximum deflection between r and q_2 which results in a change of the stiffness of the elastic element. The results are shown in figure 12. For the first simulation a maximum deflection of 0.5 rad is defined. Since 1 Nm/rad is the initial stiffness and the deflection for the initial stiffness does not exceed 0.075 rad a change of stiffness is not required for achieving a smaller deflection than the maximum defined

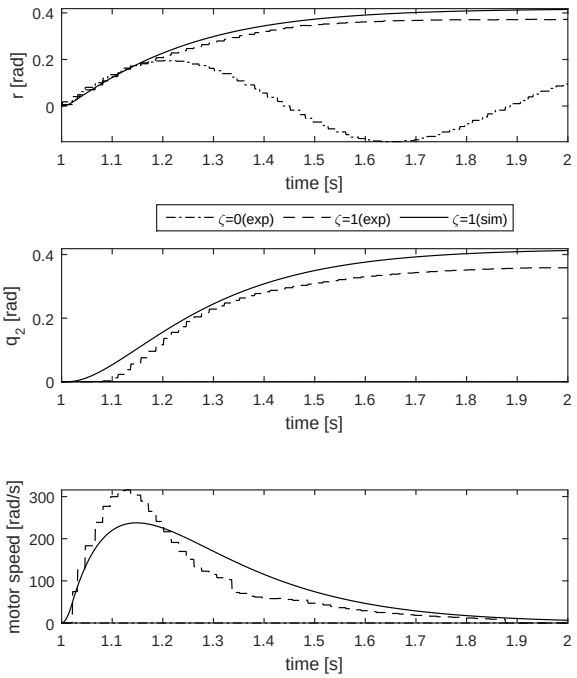

Fig. 9: Comparison of the oscillation behaviour from uncontrolled system to the controlled system. At a constant stiffness of 1 Nm/rad. The behaviour of the simulation is compared to the behaviour of the experimental set up. The iron ring hits the VSA output at $t = 1$ s.

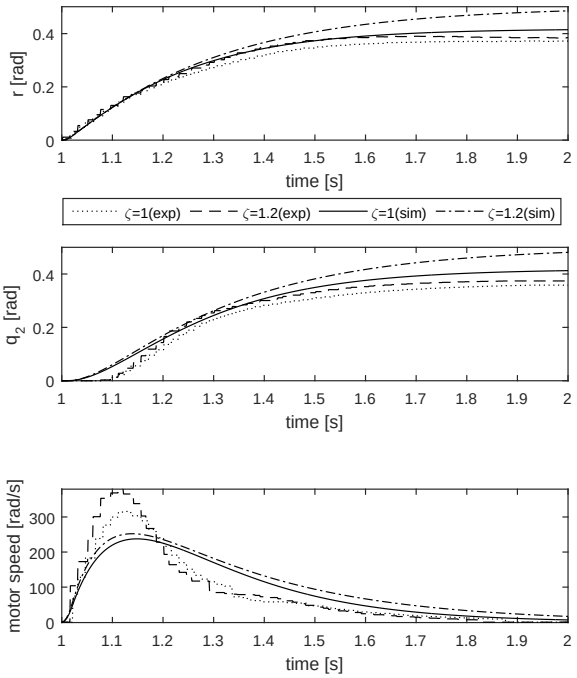

Fig. 10: Comparing an over-damped system to a critically damped system at a constant stiffness of 1 Nm/rad. Results of the simulations are compared with the results of the experimental set up. The iron ring hits the VSA output at $t = 1$ s.

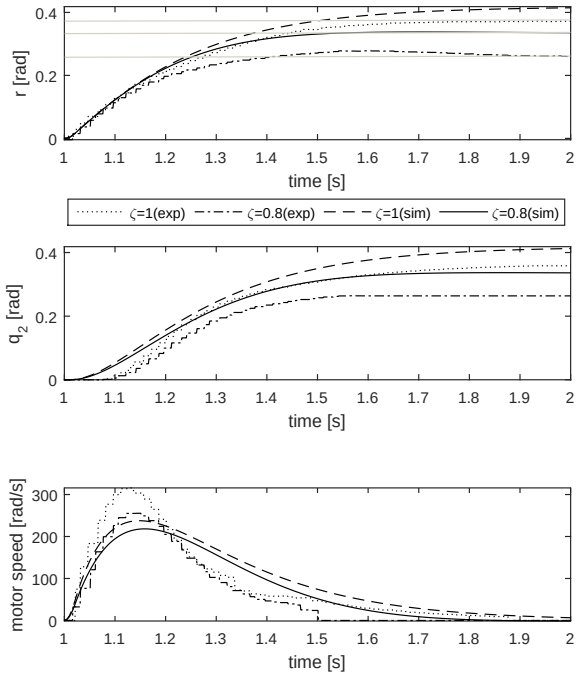

Fig. 11: Comparing an under-damped system to a critically damped system at a constant stiffness of 1 Nm/rad. Analysing the differences between simulations and the experimental set up. The iron ring hits the VSA output at $t = 1$ s.

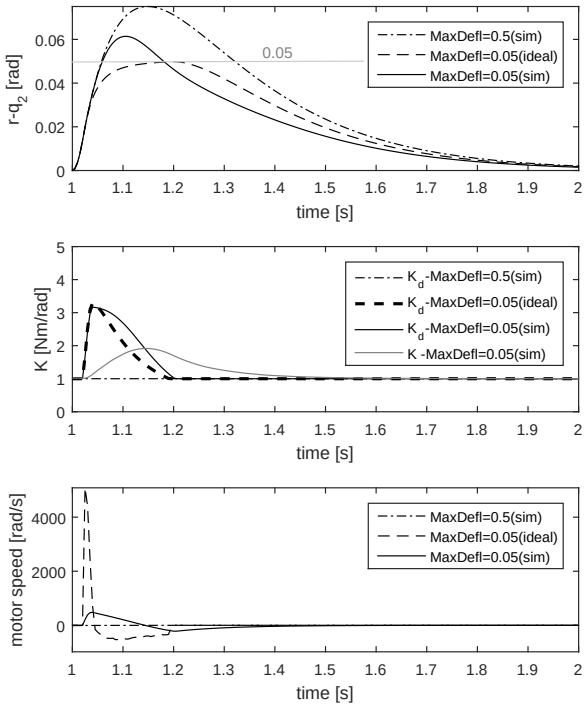

Fig. 12: Using the energy function for defining a maximum deflection of r to q_2. $K = K_{desired}$ at the idealized system. The figure shows that the idealized system is able to meet the desired behaviour by requiring a motor speed of 5000 rad/s. K and K_d lay above each other in the ideal system and in the simulation with a maximum desired deflection of 0.5 rad. Therefore only the trajectories of K_d are shown for these two simulations. The iron ring hits the VSA output at $t = 1$ s.

deflection and the stiffness stays constant at 1 Nm/rad. The second simulation is performed by assuming that the motor for changing the stiffness is ideal and therefore $K = K_{desired}$. A maximum deflection of 0.05 rad is defined. The figure shows that the stiffness gets adjusted to the total energy in the system and the deflection converges nicely to the defined maximum deflection. The ideal system where $K = K_{desired}$ would require a motor speed of 5000 rad/s whereby the maximum motor speed of the system has only a maximum motor speed of 872 rad/s. The third simulation is performed by staying within the motor limitations. Figure 12 shows that K can not follow $K_{desired}$ fast enough. The deflection is smaller than the deflection at the first simulation but compared to the ideal situation defined maximum deflection of 0.05 rad is exceeded.

IV. Discussion

The results shown in section III demonstrate that the implementation of a virtual damper for controlling a VSA leads to a definable catching behaviour of an object within the system limitations. Using the energy function for calculating the maximum deflection requires a rapid change of the stiffness of the elastic element. The dynamics of the presented experimental set up are to slow to keep the deflection smaller than the defined maximum deflection. A faster change of the stiffness by a more powerful motor or a mechanical redesign could solve this problem. The validation of the simulation shows the same behaviour due to the oscillation frequency but the gain of the friction differs from the set up to the simulation. Modelling friction is a difficult task and in this case a model by a constant parameter is probably too simple.

V. Conclusion

The paper describes a control method for catching a moving object. Therefore, a controller for a variable stiffness actuator is designed. The controller acts as virtual damper for absorbing the kinetic energy of the system. The control variables are the gain of the virtual damper and the stiffness of the elastic element. The gain of the virtual damper is scheduled on both the stiffness and the inertia of the system. The stiffness of the elastic element is chosen in order to control the maximum deflection of motor position and the position of the VSA output. Simulations and experiments were performed based on the vsaUT-II. Although the performance is limited by physical limitation of the system it was shown that the damping gain of the virtual damper can be adjusted to achieve a desired damping ratio of the system and that the deflection of the output to the motor can be controlled by the stiffness of the elastic element by considering the total energy in the system.

VI. Appendix

A. Basic model of VSA

By using the bond graph theory described in [11] a bond graph is created based on the sketch of figure 3, shown in figure 13. Since the moving object produces an impulsive

torque on the output it can be characterized by an effort source modulated by an impulse. Furthermore, because the object is rigidly attached to the output after getting in contact with it the inertia of the object J_{obj} gets added to the inertia of the output J_{load}.

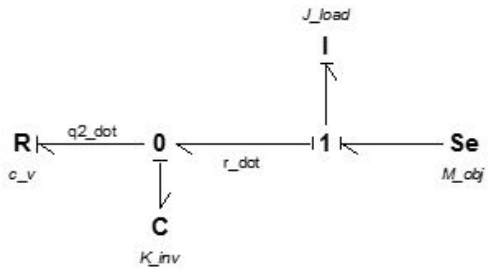

Fig. 13: Bond graph of the system sketched in figure 3. The controller acts as virtual damper c_v and therefore the motor for changing q_2 is replaced by a damping element. The environment is modelled by an effort source due to the impulsive torque input when the object hits the VSA output.

As the bond graph in figure 13 shows, the virtual damper $R : c_v$ acts as an admittance by using a torque as input for generating a flow $\dot{q}_2$ and therefore the plant acts as an impedance. In this method it is assumed that the motor including the motor controller is able to follow the desired motor speed quickly.

The system description leads to a bond graph model as shown in figure 14. For analysing the system it is assumed that $|r - q_2|$ stays small and therefore the stiffness $K(q_1)$ of the elastic element depends only on the position of the pivot point q_1, what is represented by the box around the stiffness of the elastic element $C : K_{inv}$. The dependency of K on q_1 is non-linear.

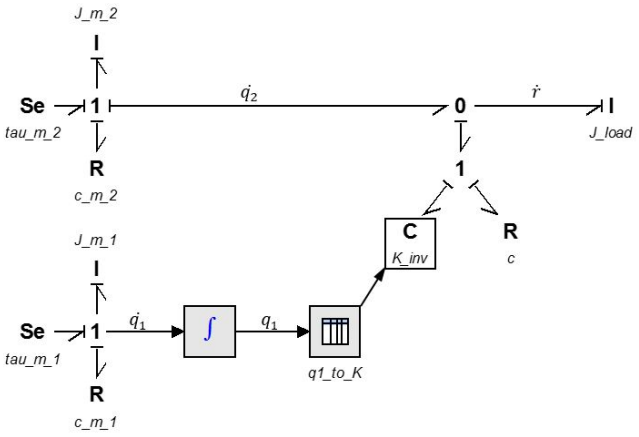

Fig. 14: Bondgraph of a VSA. The stiffness of the elastic element $\boldsymbol{K}$ has a non-linear dependency on the pivot position $\boldsymbol{q_1}$, this is represented by the Look-up table and the box around $\boldsymbol{C{:}K_{inv}}$.

The First model represents the behaviour of the main system its input is τ_{m_2} and its output is the velocity of the load r. The stiffness of the elastic element acts inside that system as a variable parameter. The state space equations (12) - (16) represent the system behaviour.

$$\dot{x} = Ax + B\tau_{m_2} \tag{12}$$

$$y = Cx \tag{13}$$

where:

$$\dot{x} = \begin{bmatrix} \frac{\partial \dot{r}}{\partial t} \\ \frac{\partial r}{\partial t} \\ \frac{\partial \dot{q_2}}{\partial t} \\ \frac{\partial \dot{q_2}}{\partial t} \end{bmatrix}; x = \begin{bmatrix} \dot{r} \\ r \\ \dot{q_2} \\ q_2 \end{bmatrix} \tag{14}$$

$$A = \begin{bmatrix} -\frac{c_{m2}+c_{m_2}}{J_{m2}} & -\frac{K}{J_{m2}} & \frac{c_{m_2}}{J_{m2}} & \frac{K}{J_{m2}} \\ 1 & 0 & 0 & 0 \\ \frac{c_{m_2}}{J_{load}} & \frac{K}{J_{load}} & -\frac{c_{m_2}}{J_{load}} & -\frac{K}{J_{load}} \\ 0 & 0 & 1 & 0 \end{bmatrix} \tag{15}$$

$$B = \begin{bmatrix} \frac{1}{J_{m2}} \\ 0 \\ 0 \\ 0 \end{bmatrix}; C = \begin{bmatrix} 1 & 0 & 0 & 0 \end{bmatrix} \tag{16}$$

The system in form of a block diagram gives the opportunity of including non-linear behaviour. This is necessary for implementing physical limitations of a system. For example maximum motor torque and maximum motor speed. Figure 15 shows the block diagram. The block diagram can be used for analysing the behaviour of a VSA without interacting with the environment.

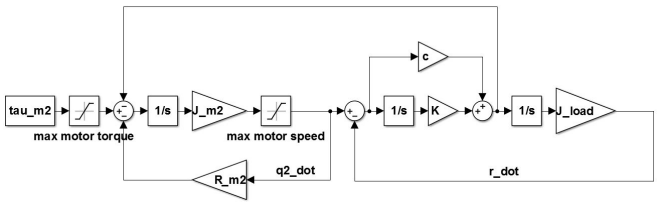

Fig. 15: Block diagram from τ_{m_2} to $\dot{r}$. Non-linear saturation elements for the physical limitations of the motor are included. The stiffness of the elastic element is modelled constant.

The simplified model shown in 15 was validated to a 20-sim experiment created by S.S. Groothuis during the system identification and parameter estimation in [12]. Therefore, the dynamics of the simplified model are compared to the 20-sim experiment by using the same impulsive input torque on the motor for changing q_2 and compare the position of the output r. This validation is performed at a stiffness of 400Nm/rad shown in figure 16 and at a stiffness of 1Nm/rad shown in figure 17. Both cases show a similar behaviour.

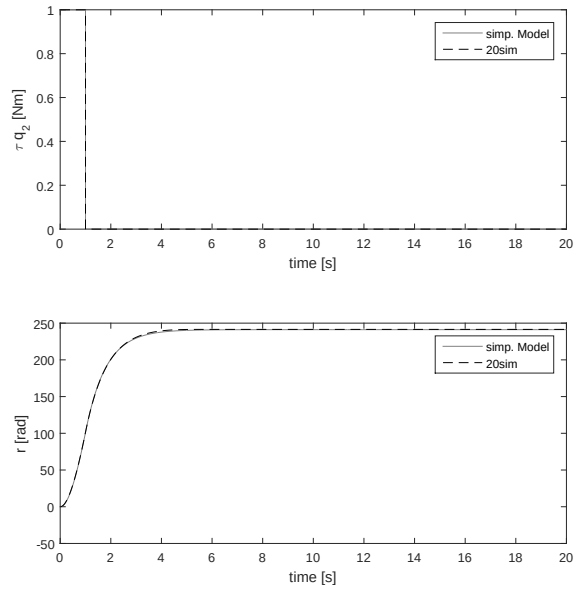

Fig. 16: Validating the dynamic behaviour of the simplified model to the 20-sim experiment at a stiffness of 400Nm/rad by applying an impulsive torque at the motor for changing q_2.

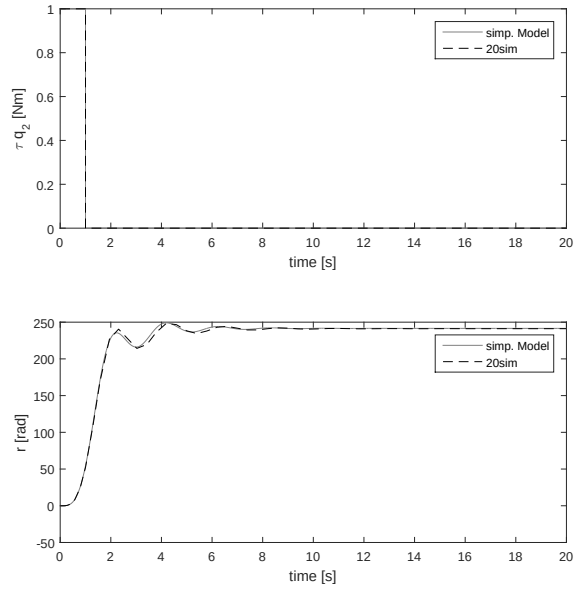

Fig. 17: Validating the dynamic behaviour of the simplified model to the 20-sim experiment at a stiffness of 1Nm/rad by applying an impulsive torque at the motor for changing q_2.

B. Calculating the inertia of the VSA output after the object is rigidly attached to the output

$$L_{cog} = \frac{m_{arm}L_{arm}/2 + m_{obj}L_{obj}}{m_{arm} + m_{obj}} \tag{17}$$

$$J_{arm2cog} = J_{arm} + m_{arm}(\frac{L_{arm}}{2} - L_{cog})^2 \tag{18}$$

$$J_{obj2cog} = J_{obj} + m_{obj}(L_{obj} - Lcog)^2 \tag{19}$$

$$J = J_{arm2cog} + J_{obj2cog} + (m_{arm} + m_{obj})L_{cog}^2 \tag{20}$$

L_{cog} is the distance of the center of gravity of the VSA output and the object to the rotation axis. $\frac{L_{arm}}{2}$ is the distance of the rotation axis and the centre of gravity of the arm and L_{obj} is the distance from the rotation axis to the center of gravity of the object.

REFERENCES

[1] H. Vallery, J. Veneman, E. v. Asseldonk, R. Ekkelenkamp, M. Buss, H. v. d. Kooij, *Compliant Actuation of Rehabilitation Robots*, in IEEE Robotics and Automation Magazine p.66-69, Vol.:15 , Issue: 3. 2008.

[2] H. Vallery, R. Ekkelenkamp, H. v. d. Kooij, M. Buss, *Passive and accurate Torque Control of Series Elastic Actuators*, in proceeding of IEEE/RSJ, p.3534-3538, International Conference on Intelligent Robots and Systems. 2007.

[3] I. Sardellitti, G. A. Medrano-Cerda, N. Tsagarakis, A. Jafari, D. G. Caldwell, *Gain Scheduling Control for a Class of Variable Stiffness Actuators Based on Lever Mechanisms*, in IEEE Transactions on Robotics, Vol.:29, Issue: 3, p. 791 - 798. 2013.

[4] L. C. Visser, R. Carloni, S. Stramigoli, *Energy Efficient Control of Robots with Variable Stiffness Actuators*, in proceedings of IEEE, p.1199-1204, IFAC Symposium on Nonlinear Control Systems. 2010.

[5] B. Buml, T. Wimböck, G. Hirzinger, *Kinematically Optimal Catching a Flying Ball with a Hand-Arm-System*, In proceeding of IEEE/RSJ, p.2592-2599, International Conference on Intelligent Robots and Systems (IROS). 2010.

[6] C. Ott, A. Albu-Schäffer, A. Kugi, G. Hirzinger, *On the Passivity-Based Impedance Control of Flexible Joint Robots*, in IEEE Transactions on Robotics Vol.:24, Issue: 2, p.416-429. 2008.

[7] T. S. Tadele, T. d. Vries, S. Stramigioli, *PID Motion Control Tuning Rules in a Damping Injection*, in proceeding of IEEE, p. 4957-4962, American Control Conference (ACC). 2013.

[8] F. Petit, A. Albu-Schäffer, *State Feedback Damping Control for a Multi DOF Variable Stiffness Robot Arm*, in proceeding of IEEE, p.5561-5567, International Conference on Robotics and Automation (ICRA). 2011.

[9] A. Albu-Schäffer, S. Wolf, O. Eiberger, S. Haddadin, F. Petit, M. Chalon, *Dynamic Modelling and Control of Variable Stiffness Actuators*, in proceeding of IEEE, p. 2155-2162, International Conference on Robotics and Automation (ICRA). 2010.

[10] R. Carloni, L. Marconi, *Limit Cycles and Stiffness Control with Variable Stiffness*, in proceedings of IEEE/RSJ, p. 5083 - 5088, International Conference on Intelligent Robots and Systems. 2012.

[11] H.M. Paynter *Analysis and design of engineering systems*, The M.I.T. Press. 1961

[12] S.S. Groothuis, G. Rusticelli, A. Zucchelli, S. Stramigoli, R. Carloni, *The Variable Stiffness Actuator vsaUT-II: Design, Modeling and Identification*, in IEEE/ASME transaction on Mechatronics, p. 589-597. 2014

[13] S.S. Groothuis, G. Rusticelli, A. Zucchelli, S. Stramigoli, R. Carloni, *The vsaUT-II: a Novel Rotational Variable Stiffness Actuator*, in proceedings of IEEE, p. 3355-3360, International Conference on Robotics and Automation (ICRA). 2012